Dielectric spectroscopy of granular material in an electrolytesolution of any ionic strength

Kirichek, Alex; Chassagne, Claire; Ghose, Ranajit

DOI
10.1016/j.colsurfa.2017.07.040

Publication date
2017

Document Version
Final published version

Published in
Colloids and Surfaces A: Physicochemical and Engineering Aspects

Colloids and Surfaces A 533 (2017) 356–370

Contents lists available at ScienceDirect

Colloids and Surfaces A

journal homepage: www.elsevier.com/locate/colsurfa

Dielectric spectroscopy of granular material in an electrolyte solution of any ionic strength

A. Kirichek*, C. Chassagne, R. Ghose

Faculty of Civil Engineering and Geosciences, Delft University of Technology, 2628 CN Delft, The Netherlands

GRAPHICAL ABSTRACT

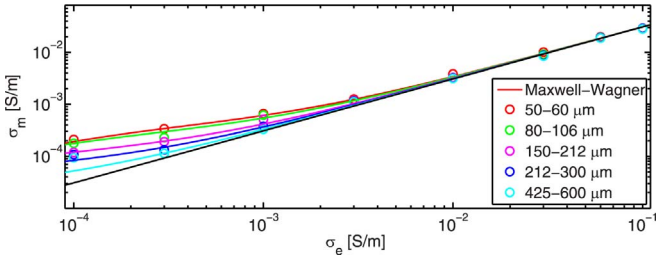

ARTICLE INFO

Keywords:
Electrokinetics
Dielectric spectroscopy
Zeta potential
Colloid

ABSTRACT

The low-frequency dielectric spectroscopy of granular material, where the porosity is representative for sands and sandstones, is until now always modeled using theories based on the work of Schwartz (1962). The theory for the low-frequency dielectric spectroscopy of suspensions, on the other hand, has been developed much further over the last decades both numerically and analytically.

In this article new analytical expressions for the complex conductivity of granular material, such as sands and sandstones in an electrolyte solution, are presented. These expressions have been derived using the theories developed for suspensions. We show that the new expressions enable to predict the measured complex conductivity of various granular material, such as packed glass beads, sands and sandstones. Because of the typical grain size of sand and sandstone particles, for any ionic strength the double layer is much thinner that the particle size. Contrary to existing theories for granular materials, the expressions we derived are valid for any ionic strength and no adjustable parameters are required.

The grains are represented by monodispersed charged spheres. We also discuss how the expressions can be adapted in the case the particles are not spherical and the grains are polydisperse.

1. Introduction

DC and AC conductivity measurements are usually performed to predict the reservoir properties of granular materials and porous rocks [1–3]. These properties are in particular: porosity, surface charge, grain or pore sizes and fluid saturation. Archie's law [4] is typically used to derive the porosity and saturation from DC measurements. In the case of AC conductivity measurements, the typical relaxation frequencies are usually obtained by using Cole–Cole type of models [5–7]. These frequencies are then linked to the grain/pore sizes [8,2].

In this article, porous media consisting of grains and electrolyte are studied. The porous media are considered to be fully saturated by the electrolyte. Compacted and uncompacted sands and sandstones can be seen as representative for these type of porous media. Percolation

* Corresponding author.

http://dx.doi.org/10.1016/j.colsurfa.2017.07.040
Received 3 May 2017; Received in revised form 5 July 2017; Accepted 11 July 2017
Available online 18 July 2017

thresholds are not considered, nor is pore clogging. Because of the typical size of the particles involved (of the order of microns), it can be estimated that one of the relaxation frequency associated with the ionic diffusion at the lengthscale of a grain is of the order of $f_a \equiv D/(2\pi a^2) \simeq$ [1–300 Hz], where $D \simeq 2 \times 10^{-9}\,\mathrm{m^2/s}$ is taken as the typical diffusion coefficient of an ion and $a \simeq$ [10–1 μm] the typical radius of a grain. This relaxation is called α relaxation by some authors [10,11]. Another relaxation exists, usually at higher frequency (depending on ionic strength and grain size), associated with the ionic diffusion at the lengthscale of the electric double layer of each grain. The corresponding relaxation, called Maxwell–Wagner–O'Konski relaxation, is also referred to as δ or β relaxation by some authors [10,11]. The Maxwell–Wagner–O'Konski relaxation frequency, often referred to as Maxwell–Wagner relaxation, is defined by $f_0 \equiv D\kappa^2/(2\pi)$ where κ^{-1} represents the double layer thickness. This thickness is given in Eq. (5) and can be estimated to give $f_0 \simeq$ [0.1–10 MHz] for monovalent salt concentrations between 0.1 mM and 10 mM. A third relaxation frequency can be associated with the polarization of water molecules. The associated relaxation frequency is termed γ relaxation [10,11] and corresponds to a strong decrease of the water dielectric permittivity in the GHz range. In the present article this relaxation is not studied as the frequency range considered is [0–10 MHz].

Models that are more elaborate than the Cole–Cole model enable to give additional information about the grain properties, such as the grain's surface charge. The surface charge of grains is an important property of the granular material as it can, for instance, be used to predict the variation of conductivity upon a pH change due to chemical reactions, or be linked to the retention and transport of contaminants and nutrients within the porous media. Current models in geophysics for granular type of porous media are based on the work of Schwartz [12], who was one of the pioneers, along with O'Konski [13,14] in setting-up the first models for the dielectric response of a colloidal particle in an applied electric field. Their models have been extended by, among others, Fixman [15,16], Hinch et al. [17] and O'Brien [18,19]. In 1981, DeLacey and White presented a full numerical model for the dielectric response of a charged sphere at any electrolyte concentration and electric field frequency [20]. In 2008, an analytical model was presented that reproduced this full numerical solution within a few percent [21]. These improved models have successfully been applied in the context of (concentrated) sediment suspensions [22–26], but never been studied in relation with porous media.

The complex conductivity of two-component mixture is usually given either in terms of Bruggeman–Hanai–Sen or Maxwell–Wagner formalisms (not to be confused with the Maxwell–Wagner relaxation introduced above). Until now, the Bruggeman–Hanai–Sen relation that includes Schwartz-like models, is used for interpreting DC and AC conductivity measurements of granular materials. The Schwartz/Bruggeman–Hanai–Sen relation has been revised by Bussian [27], to include the particle's surface conduction. In the last decade various expressions for this conduction have been proposed and tested on granular material [6,11,28].

The Bussian model however is only valid for large Dukhin numbers, which is defined in Eq. (6), and we will show how it has to be adapted for any Dukhin number. Another approach is possible, based on the Maxwell–Wagner (also named Clausius-Mossotti) relation for the complex conductivity of two-component mixture [9]. Originally the Bruggeman–Hanai–Sen and the Maxwell–Wagner relations were derived for uncharged particles. In this article we derive the corresponding relations for charged particles. We show that there is little difference between the Bruggeman–Hanai–Sen and the Maxwell–Wagner formalisms for both charged and uncharged particles. In particular, both formalisms give the same relaxation frequencies as expected.

In this article new analytical expressions for the complex conductivity of granular material, such as sands and sandstones in an electrolyte solution, are presented. These expressions are given in Eq. (9) for the Maxwell–Wagner formalism and Eq. (16) for the Bruggeman formalism. These expressions are derived using an analytical theory for the dielectric response of a colloidal particle in an applied electric field [21] that reproduces the full numerical solutions of the electrokinetic set of equations within a few percent. We show that the new expressions enable to predict the measured complex conductivity of various granular material, such as packed glass beads, sands and sandstones. Contrary to existing theories for granular materials, the expressions we derived are valid for any ionic strength and no adjustable parameters are required. The grains are represented by charged spheres and the associated electrolyte can be of any ionic strength. The particle size considered in the present study ensures that for any ionic strength $\kappa a \gg 1$. The fact that the double layers of grains overlap for low ionic strength seems to have a minor contribution to the overall conductivity as no adjustable parameters are required to predict this conductivity. We also discuss how the expressions can be adapted in the case the particles are not spherical and the grains are polydisperse.

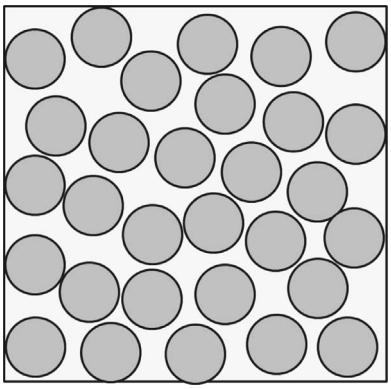

Fig. 1. The porous media is seen as packed, immobile spheres in an electrolyte.

2. Complex conductivity of granular material

In this section, new relations for the conductivity of a porous medium consisting of compacted, immobile, charged spheres are derived. As schematized in Fig. 1, we make the assumption that the spherical particles have most of their surface in contact with the electrolyte. We therefore do not consider percolation thresholds nor clogging of the interstitial cavities.

We will use $\tilde{\varepsilon}_k$ as the notation for the complex relative dielectric permittivity of substance k ($k = g$ for grains and $k = e$ for electrolyte for example). The link between the complex variables $\tilde{\sigma}_k$ (complex conductivity) and $\tilde{\varepsilon}_k$ (complex relative permittivity) is given by:

$$\tilde{\varepsilon}_k(\omega) \equiv \frac{\tilde{\sigma}_k(\omega)}{i\omega\varepsilon_0}$$

with

$$\tilde{\sigma}_k(\omega) = \sigma_k(\omega) + i\omega\varepsilon_0\varepsilon_k(\omega)$$

where σ_k is the conductivity of the studied medium, ε_k is the relative dielectric permittivity of the studied medium, ε_0 is the permittivity of vacuum, ω the applied electric field frequency and $\mathbf{i}=\sqrt{-1}$. A tilde on a symbol indicates that the corresponding variable is complex.

We define the volume fraction ϕ_s of the grains as function of the medium porosity ϕ by:

$$\phi_s = 1 - \phi = \frac{v}{V+v} \tag{1}$$

where the total volume $V + v$ is the sum of the volume of electrolyte V and the volume v of grains.

2.1. Extended Maxwell–Wagner (or Clausius–Mossotti) relation for charged spheres

The original derivation for the Maxwell–Wagner relation for uncharged spheres is given in Appendix A. In the same appendix, we discuss why the two major hypotheses we make are valid. The first hypothesis is that the grains are mainly surrounded by electrolyte which is a valid assumption as the fluid phase remains continuous to very low values of porosity [9]. We emphasize that this does not mean that the volume of electrolyte should be larger that the volume of the grains. We will show in fact that the model holds until porosities representative for sands and sandstones in Section 3. The second hypothesis is that the grains should not interact which is also a valid assumption provided that the double layers of the grains do not overlap. The particle size considered in the present study ensures that for any ionic strength $\kappa a \gg 1$. The fact that the double layers of grains overlap for low ionic strength seems to have a minor contribution to the overall conductivity as no adjustable parameters are required to predict this conductivity (see Figs. 2 and 3). When an electrical field E_0 is applied on a grain of a radius a surrounded by a double layer, both the grain and the double layer polarize. The polarization P can be written:

$$P = \tilde{\alpha} E_0 \tag{2}$$

where $\tilde{\alpha} = 4\pi\varepsilon_0\varepsilon_e a^3\tilde{\beta}$ is the polarizability and $\tilde{\beta}$ is the dipolar coefficient. Different expressions can be found in the literature for the polarizability. For instance, the polarizability of a sphere coated with a material of different dielectric constant is given by Eq. (8) in [9].

In [21] an analytical expression is given for the dipolar coefficient of a spherical charged particle in an electrolyte, which reproduces within a few percent the dipolar coefficient found by solving numerically the full set of electrokinetic equations as presented in [20]. The expression is valid for the whole range of particle's charge, ionic strength and applied field frequency. In [20,21] the colloidal particle could have an electrophoretic mobility. As stated above, in the present case, the particles are immobile. This implies that the electrophoretic term (defined as $\tilde{K}_U$ in [21]) is set equal to zero in the relation of $\tilde{\beta}$ given by Eq. (64) in [21]. Adapting Eq. (64) for the case of a non-moving sphere with a double layer thickness that is smaller than the particle size (a valid assumption for micrometric particles in nearly all experimental conditions) leads to Eq. (49) in [21] which is given by (adapting the notations to the ones used in the present article):

$$\tilde{\beta} = \frac{\tilde{\sigma}_g - \tilde{\sigma}_e + \tilde{\sigma}_{//} + \tilde{\sigma}_\perp}{\tilde{\sigma}_g + 2\tilde{\sigma}_e + \tilde{\sigma}_{//} - 2\tilde{\sigma}_\perp} \tag{3}$$

where $\tilde{\sigma}_g = i\omega\varepsilon_0\varepsilon_g$ with ε_g is the relative permittivity of the grains, $\tilde{\sigma}_e = \sigma_e + i\omega\varepsilon_0\varepsilon_e$ with ε_e and σ_e are the relative permittivity and the conductivity of the electrolyte, respectively. The complex conductivities $\tilde{\sigma}_{//}$ and $\tilde{\sigma}_\perp$ account for the parallel and perpendicular ion motion close to the grain's surface that leads to the polarization of the double layer (eventually a Stern layer contribution can also be accounted for, see Appendix C). Good approximations for $\tilde{\sigma}_{//}$ and $\tilde{\sigma}_\perp$ in the case there is no Stern layer are given by [21]:

$$\begin{aligned}\tilde{\sigma}_{//} &= \sigma_{//} = 2\frac{\sigma_e}{\kappa a}\left[\exp\left(\frac{e|\zeta|}{2kT}\right) - 1\right] \\ \tilde{\sigma}_\perp &= -\frac{J_1}{J_2}\sigma_{//}\end{aligned} \tag{4}$$

where ζ is the zeta potential of the particle, k is the Boltzmann constant and T the temperature. The relation between zeta potential and surface charge density is discussed in Appendix B. The Debye layer thickness κ^{-1} is given by

$$\kappa^{-1} = \sqrt{\frac{\varepsilon_0\varepsilon_e D}{\sigma_e}} \tag{5}$$

Furthermore

$$\begin{aligned}J_1 &= 1 + \lambda_n a \\ J_2 &= 1 + (1 + \lambda_n a)^2 \\ \lambda_n^2 &= \frac{i\omega}{D}\end{aligned}$$

where D is the typical ionic diffusion coefficient. We note from the previous expressions that the characteristic relaxation frequency associated to $\tilde{\sigma}_\perp$ is linked to the so-called α relaxation defined in the introduction, $f_a \equiv D/(2\pi a^2)$, by $|\lambda_n^2 a^2| = \omega/(2\pi f_a)$. For simplicity, we here only consider a symmetric monovalent electrolyte of valence 1 and assume that the diffusion coefficient of the cation and the anion are equal. More general expressions can be found in [21]. One generally defines

$$\mathrm{Du} = \frac{\sigma_{//}}{\sigma_e} = \frac{2}{\kappa a}\left[\exp\left(\frac{e|\zeta|}{2kT}\right) - 1\right] \tag{6}$$

The factor Du is the so-called "Dukhin number" which expresses the ratio between the parallel surface conductivity due to the ions in the double layer and the bulk conductivity. This ratio was first given by Bikerman in 1940 [29], but given the name of Dukhin who made significant progress in the work of particle polarization in electric fields in the 1970–80's [30].

A similar expression for Du is given by Eq. (37) in [31]. This Eq. (37) is also valid for non-monovalent salts and this leads to the inclusion of valences (z_k) in their expression (we use $\mathbf{z}_+ = -\mathbf{z}_- = 1$). Finally, the terms involving m_2 and Θ_2 in their expressions are corrections for the ionic velocity in the neighborhood of the particle and the contribution of the conduction of the ions in the Stern layer respectively. From Eqs. (3)–(6), one gets

$$\tilde{\beta} = \frac{\tilde{\sigma}_g - \tilde{\sigma}_e + \sigma_{//}(1 - J_1/J_2)}{\tilde{\sigma}_g + 2\tilde{\sigma}_e + \sigma_{//}(1 + 2J_1/J_2)} \tag{7}$$

In Appendix A we show that the general expression for the medium conductivity is given by

$$\tilde{\sigma}_m(\omega) = \tilde{\sigma}_e(\omega)\frac{1 + 2\phi_s\tilde{\beta}(\omega)}{1 - \phi_s\tilde{\beta}(\omega)} \tag{8}$$

The complex conductivity of the medium $\tilde{\sigma}_m$ can be obtained from measuring the current density through the porous medium for a given applied electric field. Note that no additional effects, such as electrode polarization, is accounted for here. In practice, $\tilde{\sigma}_m$ is usually obtained from 4-electrode cell measurements [41,33].

The combination of Eqs. (8) and (7) provides a new relation for the Maxwell–Wagner expression for charged spheres:

$$\tilde{\sigma}_m = \tilde{\sigma}_e\frac{[\tilde{\sigma}_g + 2\tilde{\sigma}_e + \sigma_{//}(1 + 2J_1/J_2)] + 2\phi_s[\tilde{\sigma}_g - \tilde{\sigma}_e + \sigma_{//}(1 - J_1/J_2)]}{[\tilde{\sigma}_g + 2\tilde{\sigma}_e + \sigma_{//}(1 + 2J_1/J_2)] - \phi_s[\tilde{\sigma}_g - \tilde{\sigma}_e + \sigma_{//}(1 - J_1/J_2)]} \tag{9}$$

For uncharged spheres one can show that the previous expression reduces to

$$\frac{\tilde{\sigma}_m - \tilde{\sigma}_e}{\tilde{\sigma}_m + 2\tilde{\sigma}_e} = \phi_s\frac{\tilde{\sigma}_g - \tilde{\sigma}_e}{\tilde{\sigma}_g + 2\tilde{\sigma}_e} \tag{10}$$

which is the original Maxwell–Wagner expression (Eq. (48) in Appendix A).

2.1.1. DC electric fields

In many experiments performed in geosciences, DC electric fields are traditionally used, primarily to avoid crosstalks and electromagnetic interferences within the equipment. In that case, one gets $J_1/J_2 = 1/2$. As $\sigma_g = 0$ it leads to:

$$\tilde{\beta}(\omega = 0) = \frac{-1 + \mathrm{Du}/2}{2 + 2\mathrm{Du}}$$

Assuming that Du is small (which is a reasonable assumption when κa is quite large), one gets substituting this equation into Eq. (8)

$$\sigma_m = \sigma_e \frac{1-\phi_s(1-3\mathrm{Du}/2)}{1+\phi_s(1-3\mathrm{Du}/2)/2} \tag{11}$$

This would be the conductivity of a sandstone consisting of charged spheres in an electrolyte. To obtain the porosity, the porous medium conductivity σ_m is usually fitted as function of the electrolyte conductivity σ_e according to Archie's law [4] which reads $\sigma_m = \phi^{\mathbf{m}}\sigma_e$, where $\mathbf{m}$ is an empirical coefficient, often called the cementation exponent (or index) [9], found by fitting the data. Making the equivalence between Eq. (11) and Archie's law gives the following theoretical expression for $\mathbf{m}$:

$$\mathbf{m} \equiv \ln\left[\frac{1-(1-\phi)(1-3\mathrm{Du}/2)}{1+(1-\phi)(1-3\mathrm{Du}/2)/2}\right]/\ln[\phi] \tag{12}$$

2.2. Extended Bruggeman expression for charged spheres

The Bruggeman expression is an alternative to the Maxwell–Wagner expression given the previous subsection. In order to derive the Bruggeman expression, one traditionally makes use of the Maxwell–Wagner relation Eq. (10) given for instance as Eq. (6) in Sen et al. [9]. The derivation is based on the evaluation of the mean medium conductivity $\widetilde{\sigma}_{\mathbf{n}+1}$ of a two-component mixture at a step $\mathbf{n}+1$ as function of the conductivity $\widetilde{\sigma}_{\mathbf{n}}$ at step $\mathbf{n}$. Between step $\mathbf{n}$ and $\mathbf{n}+1$, a small amount of one component is added to the mixture and therefore the mean conductivity of the medium will slightly change between the steps. A derivation can be found in Sen et al. [9]. Instead of using Eq. (10), we are going to utilize Eq. (8) in order to find a more general expression for the Bruggeman equation.

Let us assume that at step $\mathbf{n}=1$ the medium is composed of only electrolyte, thus $\widetilde{\sigma}_{\mathbf{n}=1} = \widetilde{\sigma}_e$. The initial volume occupied by the electrolyte is V. At each next step $\mathbf{n}$, a small volume dv_n of spheres and a small volume dv_e of electrolyte is added to the medium. Rewriting Eq. (8) one finds that:

$$\frac{\widetilde{\sigma}_{\mathbf{n}+1}-\widetilde{\sigma}_{\mathbf{n}}}{\widetilde{\sigma}_{\mathbf{n}+1}+2\widetilde{\sigma}_n} = \phi_{\mathbf{n}+1}\widetilde{\beta}_{\mathbf{n}} \tag{13}$$

where the grain volume fraction at step $\mathbf{n}+1$ is defined by the ratio between the volume of spheres added and the total volume. This definition stems from the derivations given in Eqs. (39)–(45), from which it follows that $dv_{\mathbf{n}} = a^3 dN$, where dN represents the number of spheres added at the step $\mathbf{n}+1$. We therefore get:

$$\phi_{\mathbf{n}+1} = \frac{\mathrm{d}v_{\mathbf{n}}}{V_{\mathbf{n}}+v_{\mathbf{n}}} \tag{14}$$

From the definition of the volume fraction Eq. (1) we get $d\phi_s = (1-\phi_s)\phi_{\mathbf{n}+1}$. Using the fact that $\bar{\sigma}_{\mathbf{n}+1} \simeq \bar{\sigma}_n$ and $\widetilde{\sigma}_{\mathbf{n}+1} - \widetilde{\sigma}_{\mathbf{n}} \equiv d\widetilde{\sigma}_{\mathbf{n}}$ we obtain from Eq. (13):

$$\frac{d\bar{\sigma}_n}{3\bar{\sigma}_n} = \frac{d\phi_s}{1-\phi_s}\widetilde{\beta}_n \tag{15}$$

The dipolar coefficient $\widetilde{\beta}_{\mathbf{n}}$ of a sphere at step $\mathbf{n}$ is found by replacing $\widetilde{\sigma}_e$ by $\widetilde{\sigma}_{\mathbf{n}}$ in Eq. (7). Combining Eqs. (15) and (7), one gets the new Bruggeman relation:

$$\left(\frac{\widetilde{\sigma}_e}{\widetilde{\sigma}_m}\right)^{\alpha}\left(\frac{\widetilde{\sigma}_m-\widetilde{\sigma}_g-\sigma_{//}(1-J_1/J_2)}{\widetilde{\sigma}_e-\widetilde{\sigma}_g-\sigma_{//}(1-J_1/J_2)}\right)^{\gamma} = \phi \tag{16}$$

with:

$$\alpha = \frac{\widetilde{\sigma}_g+\sigma_{//}(1+2J_1/J_2)}{3(\widetilde{\sigma}_g+\sigma_{//}(1-J_1/J_2))}$$

$$\gamma = \frac{\widetilde{\sigma}_g+\sigma_{//}}{\widetilde{\sigma}_g+\sigma_{//}(1-J_1/J_2)}$$

In the limit of uncharged spheres $\sigma_{//}=0$ and Eq. (16) reduces to

$$\left(\frac{\widetilde{\sigma}_e}{\widetilde{\sigma}_m}\right)^{1/3}\frac{\widetilde{\sigma}_g-\widetilde{\sigma}_m}{\widetilde{\sigma}_g-\widetilde{\sigma}_e} = \phi \tag{17}$$

which is usually referred to as the Hanai–Bruggeman–Sen formula and is equivalent to Eq. (21) in [9].

2.2.1. DC electric fields

In the DC limit one get $\widetilde{\sigma}_g = 0$ and $J_1/J_2 = 1/2$ leading to

$$\left(\frac{\sigma_e}{\sigma_n}\right)^{4/3}\left(\frac{\sigma_n/\sigma_e-\mathrm{Du}/2}{1-\mathrm{Du}/2}\right)^2 = \phi \tag{18}$$

At high ionic strengths, one expects that $Du \to 0$ and $\sigma_m = \sigma_e\phi^{3/2} < \sigma_e$ which is the limit for uncharged spheres, see [9]. By analogy with Archie's law, we then find for the cementation exponent $m = 3/2$.

2.2.2. A comment about the model of Sen et al. [9]

In [9] Sen et al. introduce the model of a self-similar rock. This model is based on the traditional Bruggeman expression Eq. (17). In their model, at each step $\mathbf{n}+1$ a small volume $dv_{\mathbf{n}}$ is added to the mixture. Like in the derivation presented above, they assume that $\widetilde{\sigma}_{\mathbf{n}=1} = \widetilde{\sigma}_e$ and the volume of electrolyte is given by V at step $\mathbf{n}=1$. The authors consider a two component mixture: one component is the electrolyte, the other is a fluid composed of electrolyte and grains. The fluid is seen as a continuum and no distinction is made between grain and electrolyte. In Sen et al.'s model, a small quantity of this fluid is added between step $\mathbf{n}$ and $\mathbf{n}+1$. The volume of component 1 (the electrolyte) is therefore not changing and remains equal to the volume V. In the derivation presented above, a small volume dv_e of electrolyte is added at each step. The fact that the volume of electrolyte is varying or not does not change the derivations given in Eqs. (13)–(17). When component 2 is seen as a continuum, it has the same properties at any scale. This enables Sen et al. to set-up their self-similar rock model, as depicted in Fig. 1 in [9].

The fact that the component made of electrolyte and grains has the same properties at any particle's radius (for a given volume fraction) is only valid in the case that the dipolar coefficient of the particles do not depend on their size. This is strictly true for uncharged spheres. In that case Eq. (7) reduces to:

$$\widetilde{\beta} = \frac{\widetilde{\sigma}_g-\widetilde{\sigma}_e}{\widetilde{\sigma}_g+2\widetilde{\sigma}_e} \tag{19}$$

which is indeed radius-independent. For charged spheres, the self-similar model is in principle not valid. In fact, for particles with different sizes but having the same surface density, we will see in Section 4 that the main contribution to the complex conductivity of the granular medium arises from the smallest particles if they are present in reasonable amount.

2.3. Comparison with the modified Vinegar and Waxman model [32,33]

A common expression for the complex conductivity $\widetilde{\sigma}_m$ of granular material is given by [32,33]

$$\widetilde{\sigma}_m = \sigma + \widetilde{\sigma}_{\mathrm{surf}} + \widetilde{\sigma}_{\mathrm{hf}} \tag{20}$$

where $\widetilde{\sigma}_{\mathrm{hf}}$ is associated to "high-frequency effects", $\widetilde{\sigma}_{\mathrm{surf}}$ to "surface conduction effects" and σ is defined by an Archie's law, $\sigma = \phi^{\mathrm{m}}\sigma_e$. In this case $\sigma_m = \mathrm{Re}(\widetilde{\sigma}_m) \neq \sigma$. This expression can be compared to the one we obtained for the Maxwell–Wagner expression for charged spheres. We rewrite the dipolar coefficient given in Eq. (7):

$$\widetilde{\beta} = \frac{-1}{2} + x \text{ with } x = \frac{3(\widetilde{\sigma}_g+\sigma_{//})}{2[\widetilde{\sigma}_g+2\widetilde{\sigma}_e+\sigma_{//}(1+2J_1/J_2)]}$$

The complex conductivity of the medium can then be rewritten from Eq. (8):

$$\widetilde{\sigma}_m = \frac{1-\phi_s}{1+\phi_s/2}\widetilde{\sigma}_e + \frac{3\phi_s x\widetilde{\sigma}_e}{1+\phi_s(1-x)+\phi_s^2(1/2-x)/2}$$

which leads to:

$$\widetilde{\sigma}_m = \frac{1-\phi_s}{1+\phi_s/2}\sigma_e + \frac{3\phi_s x\widetilde{\sigma}_e}{1+\phi_s(1-x)+\phi_s^2(1/2-x)/2} + \frac{1-\phi_s}{1+\phi_s/2}i\omega\varepsilon_0\varepsilon_e \tag{21}$$

We could therefore make the equivalence:

$$\begin{aligned}\sigma &\equiv \frac{1-\phi_s}{1+\phi_s/2}\sigma_e\\ \widetilde{\sigma}_{\text{surf}} &\equiv \frac{3\phi_s x\widetilde{\sigma}_e}{1+\phi_s(1-x)+\phi_s^2(1/2-x)/2}\\ \widetilde{\sigma}_{\text{hf}} &\equiv \frac{1-\phi_s}{1+\phi_s/2}i\omega\varepsilon_0\varepsilon_e\end{aligned} \tag{22}$$

Note that the decomposition is not unique. In the decomposition we adopted, both $\widetilde{\sigma}_{\text{surf}}$ and $\widetilde{\sigma}_{\text{hf}}$ contains high-frequency terms that are not zero. However, this decomposition is quite convenient for a better comparison with other models, as will become clear in the next subsection.

2.4. Comparison with the Bussian model

This model has originally been developed by Bussian [27] and is based on the Bruggeman expression. It describes the DC electric conductivity of a granular medium formed by charged dielectric spheres in electrolyte solution. This model, and extensions thereof, are presently widely used for interpreting complex conductivity data of porous materials [11]. We briefly recall how the Bussian model is obtained. In the text under Eq. (18), we have found that the cementation exponent is given by $\mathbf{m} = 3/2$ for uncharged spheres. Assuming that the cementation exponent will not be too different for charged spheres (which is theoretically true for small Du), Eq. (17) can be re-written:

$$\sigma_m = \sigma_e\phi^{3/2}\left(\frac{1-\sigma_g/\sigma_e}{1-\sigma_g/\sigma_m}\right)^{3/2} \tag{23}$$

see for example Appendix A of Revil and Cathles [34]. The Bussian model is obtained by introducing a particle surface conductivity σ_s, which is defined by $\sigma_g \equiv \sigma_s$. Assuming that $\sigma_s/\sigma_e \ll 1$ the Bussian model reads:

$$\sigma_m = \sigma_e\phi^{3/2}\left[1+\frac{3}{2}\frac{\sigma_s}{\sigma_e}(\phi^{-3/2}-1)\right] \tag{24}$$

Many authors (e.g. [11,28,33]) subsequently define a Dukhin number as

$$\text{Du}^* \equiv \frac{\sigma_s}{\sigma_e}$$

Let us now compare the Bussian model, based on Bruggeman, with the previous model given by Eq. (21), based on Maxwell–Wagner. Eq. (21), which is equivalent to Eq. (8), gives for DC conditions, using Eq. (22):

$$\begin{aligned}\sigma_m &= \sigma + \sigma_{\text{surf}} = \frac{1-\phi_s}{1+\phi_s/2}\sigma_e + \sigma_{\text{surf}}\\ \sigma_{\text{surf}} &\simeq \frac{9\phi_s\,\text{Du}\sigma_e}{4[1+\phi_s(1-3\text{Du}/4)]} \text{ with } \text{Du} \equiv \sigma_{//}/\sigma_e\end{aligned} \tag{25}$$

The last equivalence is obtained assuming that the term in ϕ_s^2 could be omitted in Eq. (22), which is a reasonable assumption. Comparing Eqs. (25) with Eq. (24) leads to the identification:

$$\begin{aligned}\mathbf{m} &\equiv \ln\left[\frac{\phi}{3/2-\phi/2}\right]/\ln[\phi] \simeq 3/2\\ \sigma_{\text{surf}} &\equiv \frac{3}{2}\sigma_s(1-\phi^{3/2})\end{aligned} \tag{26}$$

The approximation given in the first line of Eq. (26) can be tested using characteristic values for the porosity. For a sandstone with porosity $\phi = 0.20$ one finds $m = 1.21$ for example (for an unrealistically high porosity of $\phi = 0.50$ one gets $m = 1.32$). This gives 20% difference with $\mathbf{m} = 3/2$. This difference between the Maxwell–Wagner and the Bruggeman model can be tested at high salinities, when $Du \simeq 0$. The comparison with experimental data is done in the next section and we will see that considering the experimental error the difference between the models is not very significant. We will therefore assume that in good approximation

$$\phi^{3/2} \simeq \frac{1-\phi_s}{1+\phi_s/2} \tag{27}$$

from which we deduce, using the second line of Eq. (26), that:

$$\sigma_{\text{surf}} \simeq \frac{9}{4}\sigma_s\frac{\phi_s}{1+\phi_s/2} \tag{28}$$

Comparing Eqs. (25) and (28) leads to the identification:

$$\frac{\sigma_{//}}{\sigma_s} \equiv \frac{[1+\phi_s(1-3\text{Du}/4)]}{1+\phi_s/2} \tag{29}$$

In general there will be some difference between $\sigma_{//}$ and σ_s and only for low volume fraction (high porosity) one will have $\sigma_{//} = \sigma_s$. In that case, the relation Eq. (27) is a very good approximation.

Some authors, by extending the Bussian model, have accounted for a complex surface conductivity $\widetilde{\sigma}_s$ that they define as (see Eq. (58) in [28])

$$\widetilde{\sigma}_s \sim \frac{2}{a}\Sigma_S^* \tag{30}$$

The complex conductivity Σ_S^* is obtained from the derivation originally performed by Schwartz [12]. In Appendix D we discuss how this surface conductivity Σ_S^* is obtained and can be linked to $\sigma_{//}$. The presence of the factor 2 is also explained in the Appendix D. The conductivity $\widetilde{\sigma}_s$ has to be scaled by a as the authors in [28] express Σ_S^* as function of Γ's which are surface charge density (number/m^2) and not ionic densities (number/m^3). In Appendix D we express Σ_S^* as function of the ionic density $\tilde{n}_k$ (number /m^3).

3. Comparison with measurements

In this section the newly derived expressions for the Maxwell–Wagner and Bruggeman expressions for charged spheres are compared to experimental data. All ionic conductivities are taken equal to the values found in Handbooks. The relative dielectric permittivity of water is taken to be 80 ($\varepsilon_e = 80$) and the relative dielectric permittivity of the grain is taken to be the value for silica ($\varepsilon_g = 5$). The grains are assumed to be non conductive.

3.1. DC electric fields measurements

At low frequencies, for silica-based grains one can assume that $\widetilde{\sigma}_g = \sigma_g \ll \sigma_e$ and the Maxwell–Wagner and the Bruggeman expressions Eqs. (11) and (18) for uncharged grains ($Du = 0$) in an electrolyte reduce to

$$\begin{aligned}\sigma_m^{\text{Du}=0} &= \sigma_e\frac{1-\phi_s}{1+\phi_s/2} \text{ (MaxwellWagner)}\\ \sigma_m^{\text{Du}=0} &= \sigma_e(1-\phi_s)^{3/2}\text{(Bruggeman)}\end{aligned} \tag{31}$$

For low volume fractions, both expressions reduce to:

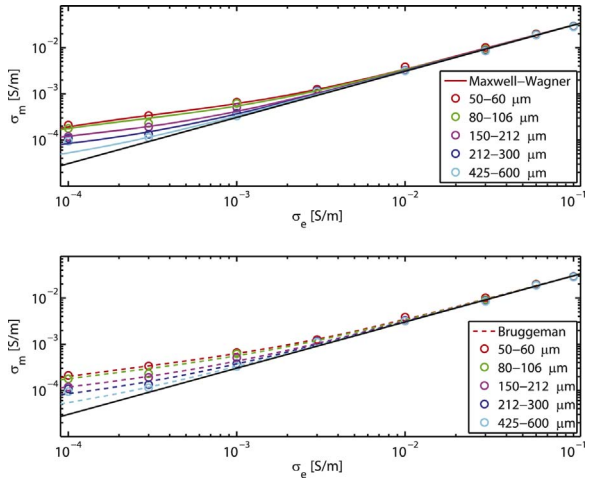

Fig. 2. Comparison between the Maxwell–Wagner and Bruggeman expressions for charged spheres using a dataset for glass beads, given in [35].

$$\frac{\sigma_m^{\mathrm{Du}=0}}{\sigma_e} = \left(1 - \frac{3}{2}\phi_s\right) \text{ for } \phi_s \ll 1 \tag{32}$$

From Archie' law, one gets:

$$\frac{\sigma_m^{\mathrm{Du}=0}}{\sigma_e} = (1-\phi_s)^{\mathbf{m}} = 1 - \mathbf{m}\phi_s \text{ for } \phi_s \ll 1 \tag{33}$$

From the equivalence it follows that $\mathbf{m} = 3/2$. Note that for the Bruggeman expression $\mathbf{m} = 3/2$ is valid for the whole range of volume fractions (for uncharged spheres). For the Maxwell–Wagner expression, the equivalence is only true at low volume fractions. For arbitrary volume fractions Eq. (12) should be used (applying $Du = 0$). In Fig. 2, we show the differences between the Maxwell–Wagner and the Bruggeman expressions in the case of glass spheres of different diameters with porosity of 0.4. The data is taken from [35]. The porosity required to fit the high ionic conductivity is 0.4 for the Maxwell–Wagner expression and 0.46 for the Bruggeman expression. For all sizes the surface charge is determined as function of ionic strength following the procedure given in Appendices B and C (see Fig. 10 in Appendix C). As can be seen from Fig. 2, for all particle sizes, the medium conductivity σ_m reduces to $\sigma_m^{\mathrm{Du}=0}$ for $\sigma_e \geqslant 10^{-2}$ S/m as expected. It is verified that for all particle sizes a surface charge value of $q = 0.0062$ C/m^2 could be used to model

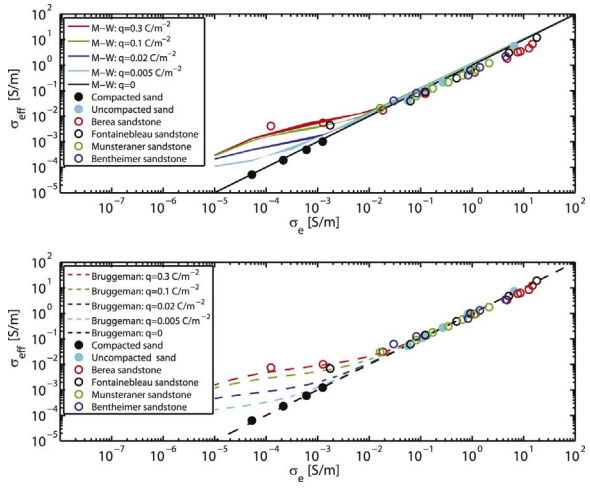

Fig. 3. Comparison between the Maxwell–Wagner and Bruggeman expressions for charged spheres. The measurements for consolidated sand, unconsolidated sand, Berea sandstone, Fontainebleau sandstone and Munsteraner sandstone are taken from [1,36,6,37,38], respectively. The conductivity of Bentheimer sandstone is measured by the authors.

the data, regardless of ionic strength. This is possible because of the small dependency of q on σ_e at low σ_e. For large σ_e the Dukhin number is in all cases in good approximation zero.

As the available measurements data presented in Fig. 3 were obtained for different porosities, we found it convenient to renormalize the data using Eq. (31) by

$$\sigma_{\mathrm{eff}} = \sigma_m / \sigma_m^{\mathrm{Du}=0}$$

This normalization ensures that at high electrolyte conductivity (where $Du = 0$) all the data should be on the $\sigma_{eff} = \sigma_e$ line. The similarly normalized Eqs. (9) and (16) are used to evaluate the theoretical curves. For all datasets, both porosity and mean particle size are known.

As can be seen in Fig. 3 there are little differences between the Maxwell–Wagner and the Bruggeman approaches. Both models reproduce quite well the data, and the values found for the surface charge are within reasonable values for silica-based grains, see Appendix B. It is also clear that for all systems investigated, the Maxwell–Wagner and the Bruggeman models for uncharged spheres can safely be used for ionic conductivities larger than 10^{-2} S/m. This is to be expected, as the grains are all about $a \simeq 10$ μm and therefore, for $\sigma_e = 10^{-2}$ S/m,

$$\kappa a \simeq a\sqrt{\frac{\sigma_e}{\varepsilon_0 \varepsilon_e D}} \simeq 850 \tag{34}$$

For the largest surface charge tested ($q = 0.3$ C/m^2), this gives $Du \simeq 0.5$.

3.2. AC electric fields measurements

Measurements in AC electric fields are quite difficult to perform as unwanted effects hamper the measurements, such as electrode polarization in the case of 2 electrodes measurements [39], or crosstalks in the case of 4 electrodes measurements [40,41].

In the present subsection, we test the Maxwell–Wagner and Bruggeman expressions for charged spheres developed in Section 2. Similarly to what was observed for DC electric fields, the Maxwell–Wagner and Bruggeman expressions give very close results in the case of AC fields, as can be observed in Fig. 4. In particular both expressions give the same relaxation frequencies, which was to be expected. As the Maxwell–Wagner relation is the one most commonly found in colloid science, we made the choice of using it in the remainder of the subsection.

We first present the prediction obtained for some measured data from [33]. The two experiments represent the dielectric response of the same sandstone of 0.40 porosity, saturated with 3 mM NaCl, at 25 °C and a pressure of 5 MPa. The experiments are done in a 4-electrode cell (experiments no 8 and 15 in [33]), before any injection of gas (hour 14 of the experiment, dark blue line in Fig. 9 of [33]). As can be seen in the figure, even though the values found are quite close in both experiments, the values of the medium conductivity differ by 9%, even though the conductivity of the electrolyte was the same in both experiments (0.037 S/m, see Table 2 in [33]). An electrolyte conductivity of 0.037 S/m corresponds roughly to a salinity of 2.5 mM NaCl. It is not clear why this salinity does not correspond to the salinity given in

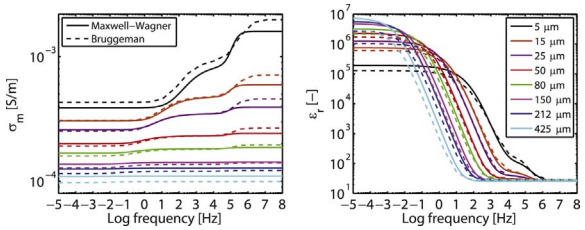

Fig. 4. Comparison between the theoretical Maxwell–Wagner and Bruggeman relations for charged spheres using various grain sizes without Stern layer, $q = 0.062$ C/m^2, $\phi = 0.4$, $\sigma_e = 0.0003$ S/m. Two relaxation frequencies can be observed: $f_a = D/(2\pi a^2)$ and $f_0 = D\kappa^2/(2\pi)$, where $f_a < f_0$ because $\kappa a \gg 1$.

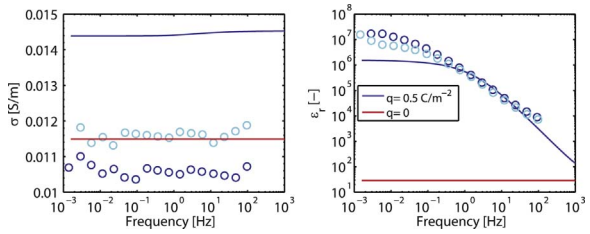

Fig. 5. Conductivity and dielectric permittivity of a sandstone saturated with 3 mM NaCl. The different colors for the symbols represent two different datasets. The red and blue solid lines show the Maxwell–Wagner relation for uncharged and charged spheres, respectively. We used $a = 20$ μm and a surface charge of 0.5 C/m^2. (For interpretation of the references to color in this figure legend, the reader is referred to the web version of this article.)

Table 2 in [33]. If the electrolyte conductivity is measured at the end of the experiment, it could be that some chemical reaction has occurred within the porous media resulting in a lowered electrolyte conductivity. As can be seen from Fig. 5, there is a good match between the dielectric permittivity data and the theoretical prediction when a value of $a = 20$ μm, a surface charge of 0.5 C/m^2 and an electrolyte conductivity of 0.037 S/m are used. At low frequencies, the theoretical prediction becomes constant, while the data shows some increase, most probably due to parasitic electrode effects or crosstalks of 4 electrodes. At the highest measured frequencies some deviation also occurs that can be due to some unaccounted crosstalks. The electric conductivity found using the expression for charged spheres is slightly higher (by 20%) than the measured one, which is closer to the conductivity found using the expression for uncharged spheres. We did not try to improve the fit, which would be possible by accounting for a Stern layer for example (see Appendix B), as we tried to keep the amount of adjustable to a minimum.

Recently, experiments were presented that were performed on a Portland sandstone which contained some amount of illite and kaolinite as function of frequency, for a large range of ionic strength [41]. In that article, the measurements were analyzed using an extended Bussian model making use of a Schwartz-like surface conductivity. We refer to [41] and references within for further details. From the low-frequency data given in [41] a relation between the medium and electrolyte conductivity, given in Fig. 6a, was found that enabled to estimate the Dukhin number Du, see Fig. 6b, using Eq. (11). We note that if we would use the porosity given by the authors ($\phi = 0.2$) Du becomes negative at high ionic conductivities, which is the consequence of the fact that the medium conductivity would then be larger than the conductivity of a comparable medium (in terms of same porosity and particle size) but composed of uncharged spheres, which is theoretically impossible. This is reflected in the crossing of the full blue curve and the experimental curve (red circles) in Fig. 6a. For most of the experimental data given in Fig. 3, it is also usually found that the Maxwell–Wagner expression for uncharged spheres gives slightly higher values than the measured ones at high salinity, and that the Bruggeman expression for charged spheres performs better. We have to adjust the porosity to 0.05 in order to get a positive Dukhin number. This last value is not realistic,

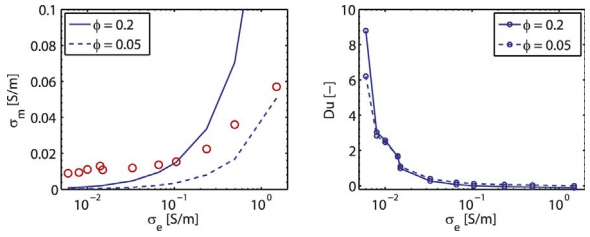

Fig. 6. Estimation of Du from measured data. The values obtained for Du for 0.2 porosity are given in Table 1 as $Du(\sigma_m)$ using Du and a as adjustable parameters. (a) $Du(\sigma_m)$ used as fit; (b) $Du(\varepsilon_m)$ used as fit.

Table 1
Values used in the model (see text for details).

σ_e (S/m)	0.105	0.033	0.015	0.014
a (μm)	7	7	7	7
ε_e	5000	6000	4000	7000
Du (ε_m)	0.2461	0.3214	0.4999	0.6095
q_0 (C/m^2)	1.2	0.5	0.35	0.4
Du (σ_m)	0.0031	0.2699	0.9753	1.6444
q_0 (C/m^2)	0.02	0.4	0.65	1.03

but as can be seen in Fig. 6b the Du numbers found from using porosities $\phi = (1 - \phi_s)$ of 0.2 and 0.05 are quite close for the lowest conductivities. This can be understood by realizing that for low frequencies and for large Du Eq. (9) gives:

$$\sigma_m \simeq \sigma_e \frac{1 + \mathrm{Du}(1 + \phi_s/2)}{1 + \mathrm{Du}(1 - \phi_s/4)}$$

which gives quite small differences for σ_m for volume fractions ϕ_s between 0.8 and 0.95. In the remainder of this subsection, the porosity will be kept equal to 0.20.

Some of the data given in [41] is replotted and fitted according to the Maxwell–Wagner expression for charged spheres. Again, we tried to keep the number of adjustable variables as minimal as possible. As recognized by [41] (their comment in the legend of their Fig. 5), some artifacts are observed at very low and very high frequency. Like for the data of [33], parasitic electrode effects or crosstalks of 4 electrodes are present at very low frequencies, resulting in an increase in the dielectric permittivity with decreasing frequencies, whereas a constant value is expected. At high frequencies, other unwanted effects took place, resulting in unrealistic high values for the dielectric permittivity. In order to account for these high-frequencies effects, we adjusted the dielectric permittivity of the electrolyte in the variable $\tilde{\varepsilon}_e$ for each salinity to match the model prediction with the high frequency value of the sandstone permittivity. The values used in the model are given in Table 1. Two types of fits are performed. In Fig. 7a, we show the result of the low frequency fit of the conductivity done by adjusting $Du(\sigma_m)$ and in Fig. 7b we show the result of the dielectric permittivity fit done by adjusting $Du(\varepsilon_m)$. A value of 7 μm is found to be the best grain size for all the fits. The value of q_0 given in Table 1 could then be calculated from $Du(\sigma_m$ or $\varepsilon_m)$, a and σ_e. The model clearly does not reproduce the features of the 0.105 S/m data for either the Du (ε_m) or the Du (σ_m) fit. For lower ionic conductivities, the model gives reasonable predictions. Note however the large difference between the fit parameters for the

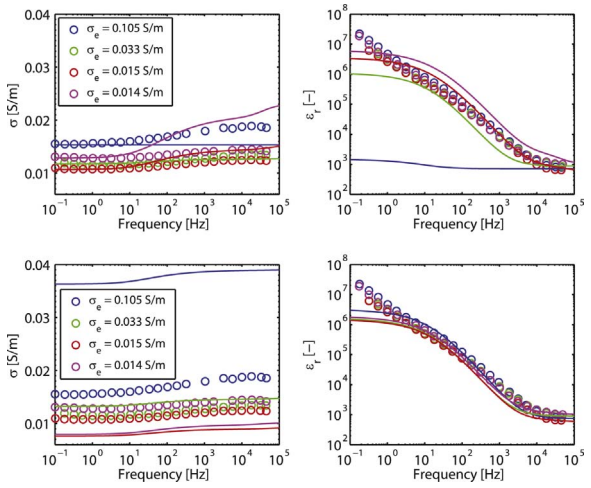

Fig. 7. Comparison of measured data and the Maxwell–Wagner expression for charged spheres.

0.015 and 0.014 S/m conductivity data. They arise from the unexpected large differences between the conductivities for these datasets.

4. Models for non-spherical and polydisperse spheres

In the previous section we have shown that the Maxwell–Wagner and Bruggeman expressions for charged spheres enable to estimate reasonably correctly the different amplitudes and relaxation frequencies of the complex conductivity of granular systems. The fits were not perfect for several reasons. One reason is the uncertainty of the measurement data. Dielectric spectroscopy measurements are very difficult to perform accurately at low and high frequencies for many technical reasons. From the results of the previous section, it can be seen that even small deviations for the conductivity data results in large changes in the fit results. High frequency inaccuracies in the dielectric permittivity increment (resulting from inaccuracies in the phase measurement), on the other hand, can better be compensated for. The other reasons for the discrepancies between the model and the data stem from the model. In particular, the model was derived assuming that the particles were all monodisperse spheres. Sandstones can contain polydisperse and/or non-spherical particles. In the present section we will briefly discuss on how to account for non-sphericity and polydispersity.

4.1. Non-spherical particles

The dipolar coefficient Eq. (3) that was used to set-up both the Maxwell–Wagner and the Bruggeman expressions for charged spheres can quite easily be extended for charged spheroidal particles. Such general expression is given as Eq. (1) in [21]. Sen et al. give in the Appendix of [9] similar expressions for uncharged spheroidal particles and the associated the Bruggeman expression. Clays can in first approximation be considered to be either prolate or oblate spheroids [45]. The dipolar coefficients for other geometries are also available [42,43].

4.2. Polydisperse samples

The Maxwell–Wagner and the Bruggeman expressions for charged spheres can easily be extended to account for polydispersity. Let us assume that the granular material is polydisperse. For the sake of argument we only consider a granular material composed of two types of grains (labeled 1 and 2), but the reasoning be extended to more classes of particles in a straightforward manner. A relation between the different volume fractions is given by:

$$1 = \frac{V_{\text{tot}}}{V_{\text{tot}}} = \frac{V_w + V_1 + V_2}{V_{\text{tot}}} = \phi_s^w + \phi_s^1 + \phi_s^2 = \phi_s^w + \phi_s \tag{35}$$

where ϕ_s^w, ϕ_s^1, ϕ_s^2 represent the volume fractions of water, particle of type 1 and particles of type 2. Eq. (8) gives:

$$\widetilde{\sigma}_m = \widetilde{\sigma}_e \frac{1 + 2[\phi_s^1 \widetilde{\beta}_1 + \phi_s^2 \widetilde{\beta}_2]}{1 - [\phi_s^1 \widetilde{\beta}_1 + \phi_s^2 \widetilde{\beta}_2]} \tag{36}$$

Each dipolar coefficient can be written:

$$\widetilde{\beta}_k(\omega = 0) \simeq \frac{-1}{2}\left(1 - \frac{3}{2}\text{Du}_k\right) \tag{37}$$

which enables to derive the DC conductivity of the polydisperse granular medium:

$$\sigma_m = \frac{1 - \phi_s}{1 + \phi_s/2}\sigma_e + \frac{9(\phi_s^1 \text{Du}_1 + \phi_s^2 \text{Du}_2)\sigma_e}{4\left[1 + \phi_s - \frac{3}{4}(\phi_s^1 \text{Du}_1 + \phi_s^2 \text{Du}_2)\right]} \tag{38}$$

From this equation it appears that the second term on the right-hand-side will be dominated by the particle type displaying the highest product ($\phi_s Du$). This could particularly important in the case of shale sands as the clay fraction particles have typically a smaller size and higher charge than the sand particles. If their volume fraction ϕ_s is large enough, the medium conductivity σ_m at low salinities will therefore be dominated by the clay fraction.

5. Conclusion

The low-frequency dielectric spectroscopy (complex conductivity) of granular material, where grains are typically of micrometer size and porosity representative for sands and sandstones, is until now always modeled using theories based on the work of Schwartz [12]. The Schwartz theory has been incorporated in the Bruggeman–Hanai–Sen relation to yield the complex conductivity. This Schwartz/Bruggeman–Hanai–Sen relation has been revised by Bussian [27], to include the particle's surface conduction. Models have been derived over the last decades giving expressions for this conduction and incorporated in the model of Bussian [6,28,11]. Alternatively, a general model Eq. (20), that we show can be linked to the Maxwell–Wagner relation, has been proposed and tested on granular material [32,33,41]. None of these models properly accounts for the polarization of a charged particle in an electric field as the model of Schwartz only reproduces the numerical solution found by solving the complete set of electrokinetic equations [20] for frequencies such that $f \gg f_a \equiv D/(2\pi a^2)$ (see Appendix D).

In 2008, an analytical model was presented that reproduced this full numerical solution within a few percent [21]. This model has successfully applied to suspensions [22,24,25,45]. In the present article, this model is incorporated into the Bruggeman–Hanai–Sen and Maxwell–-Wagner relations. We show that there is little difference between the Bruggeman–Hanai–Sen and the Maxwell–Wagner formalisms for both charged and uncharged particles. In particular, both formalisms give the same relaxation frequencies as expected. The Maxwell–Wagner relation for charged spheres is tested on available data from the literature. We show that the new expressions enable to predict the measured complex conductivity of various granular material, such as packed glass beads, sands and sandstones. Contrary to existing theories for granular materials, the expressions we derived are valid for any particle size, ionic strength, electric field frequency and no adjustable parameters are required. All parameters can be assessed independently.

The main assumption made in deriving the theory is that the polarization of each grain is not much influenced by its neighbors. We show that this condition is not restrictive for the data discussed in this article. Percolation thresholds are not considered, nor is pore clogging. This implies that the models are valid for porous media in which each particle (grain) has nearly all of its surface in contact with the electrolyte. In the last section we discuss how the model should be adapted in the case the particles are of a different size, different shape and/or have a different surface charge. This extended model should be tested on for examples shaly sands to prove, as we discussed in Section 4, that the main contribution to the medium complex conductivity arises from the particles for which the product ($\phi_s Du$) is highest.

Acknowledgements

This research has been carried out in the context of the CATO2 program with grant number FES10036GXDU. CATO2 is a Dutch National Research Program on Carbon Capture and Storage (CCS) Technology. The program is financially supported by the Dutch Government (Ministry of Economic Affairs) and the CATO2 consortium parties.

Appendix A. Maxwell–Wagner (or Clausius–Mossotti) relation for uncharged spheres

We recall how the Maxwell–Wagner relation is derived, as this enables to understand how this relation can be adapted to account for the

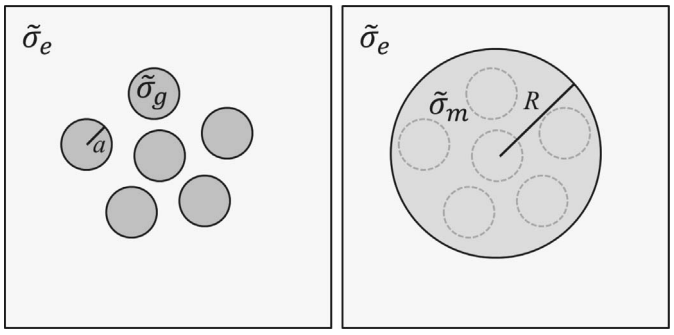

Fig. 8. Left: spheres with radius a of complex conductivity $\tilde{\sigma}_g$ in an electrolyte solution of complex conductivity $\tilde{\sigma}_e$. Right: equivalent medium with characteristic lengthscale R of complex conductivity $\tilde{\sigma}_m$ in an electrolyte solution of complex conductivity $\tilde{\sigma}_e$.

polarization of the grains under the influence of the applied electric field E. The full derivations can be found in [46,47]. Spherical coordinates (r, Θ, φ) are used.

We consider a system consisting of N non-interacting spheres. Each sphere, which has a complex conductivity $\tilde{\sigma}_g$ (equivalently the complex permittivity is $\tilde{\varepsilon}_g$) and a dipolar coefficient $\tilde{\beta}$, is embedded in a medium of complex conductivity $\tilde{\sigma}_e$ (equivalently the complex permittivity is $\tilde{\varepsilon}_e$). The electric potential at a given distance of the dipoles is given by:

$$\tilde{\Psi}_{\text{out}} = -\mathbf{E}\cdot\mathbf{r}\left[1 - N\tilde{\beta}\left(\frac{a}{r}\right)^3\right] \tag{39}$$

where a is the characteristic radius of a particle having a dipolar coefficient $\tilde{\beta}$. One can also represent the system consisting of N dipoles and its surrounding fluid as being an homogeneous medium of dipolar coefficient $\tilde{\beta}_m$ and complex conductivity $\tilde{\sigma}_m$, as depicted in Fig. 8. In this case we get for the electric potential outside this medium:

$$\tilde{\Psi}_{\text{out}} = -\mathbf{E}\cdot\mathbf{r}\left[1 - \tilde{\beta}_m\left(\frac{R}{r}\right)^3\right] \tag{40}$$

where R is the characteristic length of pseudo-homogeneous medium of complex conductivity $\tilde{\sigma}_m$. Laplace equation can be applied to the interior of the pseudo-homogeneous medium:

$$\Delta\tilde{\Psi}_{\text{in}}(r < R) = 0 \tag{41}$$

yielding

$$\tilde{\Psi}_{\text{in}}(r < R) = A \times \mathbf{E}\cdot\mathbf{r} \tag{42}$$

where A is an integration constant. This constant can be eliminated using the standard boundary conditions:

$$\tilde{\sigma}_m\left(\frac{\partial\tilde{\Psi}_{\text{in}}}{\partial r}\right)_{r=R} = \tilde{\sigma}_e\left(\frac{\partial\tilde{\Psi}_{\text{out}}}{\partial r}\right)_{r=R}$$
$$\tilde{\Psi}_{\text{in}}(R) = \tilde{\Psi}_{\text{out}}(R) \tag{43}$$

and one finds:

$$\tilde{\beta}_m = \frac{\tilde{\sigma}_m - \tilde{\sigma}_e}{\tilde{\sigma}_m + 2\tilde{\sigma}_e}\left(=\frac{\tilde{\varepsilon}_m - \tilde{\varepsilon}_e}{\tilde{\varepsilon}_m + 2\tilde{\varepsilon}_e}\right) \tag{44}$$

Equating Eqs. (39) and (40) leads to:

$$\tilde{\beta}_m = \tilde{\beta}\frac{\text{Na}^3}{R^3} = \tilde{\beta}\phi_s \tag{45}$$

where ϕ_s is the volume fraction associated to the N particles. We then obtain Eq. (8)

$$\tilde{\sigma}_m(\omega) = \tilde{\sigma}_e(\omega)\frac{1 + 2\phi_s\tilde{\beta}(\omega)}{1 - \phi_s\tilde{\beta}(\omega)} \tag{46}$$

In order to obtain the traditional Maxwell–Wagner relation, it is necessary to assume that

$$\tilde{\beta} = \frac{\tilde{\sigma}_g - \tilde{\sigma}_e}{\tilde{\sigma}_g + 2\tilde{\sigma}_e} \tag{47}$$

a relation that is valid for an uncharged sphere of complex conductivity $\tilde{\sigma}_g$ [21]. Eqs. (46) and (47) lead to

$$\frac{\tilde{\sigma}_m - \tilde{\sigma}_e}{\tilde{\sigma}_m + 2\tilde{\sigma}_e} = \phi_s\frac{\tilde{\sigma}_g - \tilde{\sigma}_e}{\tilde{\sigma}_g + 2\tilde{\sigma}_e} \tag{48}$$

This relation is given as Eq. (6) in Sen et al. [9]. As stated by Sen et al. under their Eq. (6), the Maxwell–Wagner relation is also known as the Clausius-Mossotti or Maxwell–Garnett relation. In most experimental studies the core material of a colloidal particle can be considered as purely

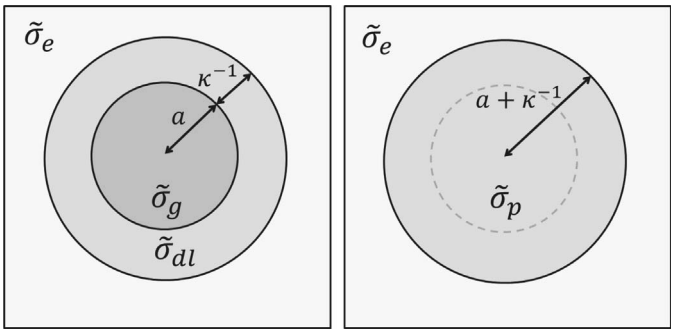

Fig. 9. Left: spherewith radius a of complex conductivity $\tilde{\sigma}_g$ with a double layer of complex conductivity $\tilde{\sigma}_{\mathrm{dl}}$ in an electrolyte solution of complex conductivity $\tilde{\sigma}_e$. Right: equivalent sphere of radius $a + \kappa^{-1}$ of complex conductivity $\tilde{\sigma}_p$ in an electrolyte solution of complex conductivity $\tilde{\sigma}_e$.

dielectric (non-conducting). This is the case for most silica-based particles for example. The medium can then be seen as an electrolyte solution in which there are the dielectric holes. Eq. (48) leads to, assuming $\sigma_g = 0$:

$$\begin{aligned}\sigma_m &= \sigma_e \frac{2(1-\phi_s)}{2+\phi_s} \\ &= \sigma_e \text{ for } \phi_s \ll 1\end{aligned} \tag{49}$$

For low volume fractions, the medium conductivity is in good approximation equal to the conductivity of the electrolyte.

Alternatively, it is possible to consider the system as N spheres of complex conductivity $\tilde{\sigma}_e$ embedded in an medium of complex conductivity $\tilde{\sigma}_g$. The porous media in this case is an insulating medium in which there are pockets of electrolyte. One then gets:

$$\frac{\tilde{\sigma}_m - \tilde{\sigma}_g}{\tilde{\sigma}_m + 2\tilde{\sigma}_g} = (1-\phi_s)\frac{\tilde{\sigma}_e - \tilde{\sigma}_g}{\tilde{\sigma}_e + 2\tilde{\sigma}_g} \tag{50}$$

This last equation leads to, assuming $\sigma_e \gg \sigma_g$:

$$\begin{aligned}\sigma_m &= \sigma_g \frac{1+2(1-\phi_s)}{1-(1-\phi_s)} \\ &= 0 \text{ for } \sigma_g = 0\end{aligned} \tag{51}$$

This last relation implies that the medium is not conducting.

In the case of sands and sandstones, one would be tempted to prefer Eq. (50) over Eq. (48), as intuitively there are more sand grains than water in these systems. However, the restrictions imposed on Eq. (48) do not depend on the volumetric ratio between grains and water. The two major hypotheses made to derive Eq. (48) are: (a) the grains are surrounded by electrolyte (this does not mean that the volume of electrolyte should be more important than the volume of grains) and (b) the interactions between grains are neglected. As discussed by Sen et al., the pore space remains connected in the first order of approximation in most experimental studies, with the grains touching each other only at or on small, isolated regions of contact (see p. 784/785 in [9]). This implies that the fluid phase remains continuous to very low values of the porosity (very high values of the volume fraction) and this validates hypothesis (a). As for hypothesis (b), the major consequence of dipole-dipole interaction is usually that the dipoles tend to re-orient in the electric field, bringing particles in contact along the electric field lines. This movement is not possible in sand, as the particles are too large and too compacted to move. Multipole effects can most probably be neglected as well in first approximation and therefore hypothesis (b) should be quite measurable. Hypotheses (a) and (b) enable to approximate the porous medium as a concentrated suspension of (spherical) grains which are immobile. Each grain is assumed to have the same dipolar coefficient as it would have without the presence of its neighbors.

A.1 The shell model

The same mathematical derivations as given in Eqs. (39)–(46) can be applied to evaluate the mean complex conductivity of a charged sphere surrounded by an electric double layer. The model then obtained is called the shell model [48]. A sketch is given in Fig. 9.

Following the same lines of derivations as above, one can show that:

$$\frac{\tilde{\sigma}_p - \tilde{\sigma}_{\mathrm{dl}}}{\tilde{\sigma}_p + 2\tilde{\sigma}_{\mathrm{dl}}} = \phi_{\mathrm{dl}} \frac{\tilde{\sigma}_g - \tilde{\sigma}_{\mathrm{dl}}}{\tilde{\sigma}_g + 2\tilde{\sigma}_{\mathrm{dl}}}$$

where $\tilde{\sigma}_{\mathrm{dl}}$ is the complex conductivity associated to the double layer, $\tilde{\sigma}_p$ is the complex equivalent conductivity of the system consisting of the grain and its double layer (p stands for "particle" in the broad sense) and ϕ_{dl} is the volume fraction associated to the double layer of thickness κ^{-1}, hence:

$$\phi_{\mathrm{dl}} = \frac{a^3}{(a+\kappa^{-1})^3} = \frac{1}{(1+1/(\kappa a))^3} \simeq 1 - \frac{3}{\kappa a} \text{ (for large } \kappa a)$$

Subsequently the dipolar coefficient of the particle (grain and double layer) can be evaluated from:

$$\tilde{\beta} = \frac{\tilde{\sigma}_p - \tilde{\sigma}_e}{\tilde{\sigma}_p + 2\tilde{\sigma}_e} \tag{52}$$

The analogy between Eqs. (7) and (52) was already pointed out in [48]. Note that the shell model does not account for the distortion of the double

layer (or any other layer) under the influence of the electric field, but only its polarization. This implies that the shell model is only valid for large κa. Additional layers can similarly be added, accounting for example for a Stern layer complex conductivity. This is discussed in Appendix C.

Appendix B. pH dependence of the surface charge

The electric surface potential of the particle can be linked to its surface charge which is a measurable quantity (by titration for example). The relation between surface charge density $q_{eq}(a)$ and potential $\Psi_{eq}(a)$ is given by Gauss' law:

$$\left(\frac{\partial \Psi_{\mathrm{eq}}}{\partial r}\right)_{r=a} = \frac{-q_{\mathrm{eq}}(a)}{\varepsilon_0 \varepsilon_e} \tag{53}$$

Solving this equation requires to solve the non-linear Poisson-Boltzmann equation, however there exists a very good approximation for symmetric monovalent electrolytes [49]:

$$q_{\mathrm{eq}}(a) = \frac{\varepsilon_0 \varepsilon_e \mathrm{kT}}{e} \kappa \left[2 \sinh\left(\frac{e\Psi_{\mathrm{eq}}(a)}{2\mathrm{kT}}\right) + \frac{4}{\kappa a} \tanh\left(\frac{e\Psi_{\mathrm{eq}}(a)}{4\mathrm{kT}}\right)\right] \tag{54}$$

In most cases encountered experimentally $\kappa a \gg 1$ and Eq. (54) can be simplified to provide an expression for $\Psi_{eq}(a)$:

$$\frac{e\Psi_{\mathrm{eq}}(a)}{\mathrm{kT}} = 2\,\mathrm{asinh}\left(\frac{\mathrm{eq}_{\mathrm{eq}}(a)}{2\varepsilon_0 \varepsilon_e \mathrm{kT}\kappa}\right) \tag{55}$$

We emphasize that $q_{eq}(a)$ is the surface charge density in the absence of any applied electric field and that this surface charge can be pH/pK dependent. From the value of q_{eq}(pH, pK) the zeta potential ζ(pH, pK) can be back-calculated assuming that (1) there is no Stern layer and (2) the shear plane is located at $r = a$ from which one gets

$$\Psi_{\mathrm{eq}}(a) = \zeta \tag{56}$$

The salt-concentration dependence in Eq. (54) through the term κ reflects the presence of the double-layer close to the particle's surface, i.e. the presence of indifferent ions (ions that do not chemically interact with the surface).

The surface charge $q_{eq}(a)$ can be given in terms of charge dissociation parameters. For simplicity, we will consider only one surface dissociation, given by the generic formulation:

$$-\mathrm{AH} = -A^- + H^+ \tag{57}$$

The corresponding mass action law for the surface equilibrium is given by:

$$a_{H^+} \frac{\Gamma_{A^-}}{\Gamma_{\mathrm{AH}}} = K \exp\left(\frac{e\Psi_{\mathrm{eq}}(a)}{\mathrm{kT}}\right) \tag{58}$$

where

$$\begin{aligned} \mathrm{pH} &= -\log(a_{H^+}) \\ \mathrm{pK} &= -\log(K) \end{aligned} \tag{59}$$

The total concentration of surface sites reads:

$$\Gamma^0 = \Gamma_{A^-} + \Gamma_{\mathrm{AH}} \tag{60}$$

where the surface charge density originating from the dissociated groups reads:

$$q_{\mathrm{eq}}(a) = -e\Gamma_{A^-} \tag{61}$$

Combining the previous equations leads to:

$$\Gamma^0 = \Gamma_{A^-}\left[1 + \frac{10^{-\mathrm{pH}}}{K \exp(e\Psi_{\mathrm{eq}}(a)/\mathrm{kT})}\right] \tag{62}$$

Note that usually one defines [50]

$$\Psi_N = \frac{\mathrm{kT}}{e}[\mathrm{pK} - \mathrm{pH}]\ln(10) \tag{63}$$

in which case it is possible to write:

$$\Gamma^0 = \Gamma_{A^-}\left[1 + \frac{1}{\exp(e[\Psi_{\mathrm{eq}}(a) - \Psi_N]/\mathrm{kT})}\right] \tag{64}$$

from which one gets:

$$q_{\mathrm{eq}}(a) = \frac{-e\Gamma^0 \exp(e[\Psi_{\mathrm{eq}}(a) - \Psi_N]/\mathrm{kT})}{\exp(e[\Psi_{\mathrm{eq}}(a) - \Psi_N]/\mathrm{kT}) + 1} \tag{65}$$

In order to solve this equation, one needs an additional equation for $\Psi_{eq}(a)$. This relation is provided by Eq. (54) which links $\Psi_{eq}(a)$ and $q_{eq}(a)$.

Appendix C. Inclusion of a Stern layer

Ions in the Stern layer can also contribute to the medium conductivity and will also depend on the existing dissociated surface sites. However, expressions for including a Stern layer contribution will depend on several factors that are difficult, if not impossible to quantify. To name a few: the exact position of the shear plane (defining which ions in the Stern layer will be mobile or not), the mobility of the ions in the Stern layer (which is most probably different from their bulk mobility), the spatial extension of the chemisorbed ions (which will define the inner and outer Helmholtz plane) [51]. This is why the Stern layer conductivity (which can be in theory a complex number i.e. frequency-dependent) is usually chosen to be an adjustable variable and included in the dipolar coefficient as an additional shell layer, see subsection the shell model in Appendix A .

In the traditional description of the Stern layer however, the Stern layer is seen as a dielectric medium, with no conductivity. The Stern model is in this case used to improve the prediction of the surface charge measured by titration (in the absence of applied electric field). One relates the surface potential $\Psi_{eq}(a)$ to the electric potential at the beginning of the diffuse layer $\Psi_{eq}(a+d)$ by an unknown Stern layer capacitance C_{Stern}

$$C_{\text{Stern}} = \frac{q_{\text{eq}}(a)}{\Psi_{\text{eq}}(a) - \Psi_{\text{eq}}(a+d)} \tag{66}$$

When this occurs Eq. (54) should be changed into:

$$q_{\text{eq}}(a+d) = \frac{\varepsilon_0 \varepsilon_e \text{kT}}{e} \kappa \left[2\sinh\left(\frac{e\Psi_{\text{eq}}(a+d)}{2\text{kT}} \right) + \frac{4}{\kappa a} \tanh\left(\frac{e\Psi_{\text{eq}}(a+d)}{4\text{kT}} \right) \right] \tag{67}$$

as $q_{eq}(a+d)$ now represents the surface charge at the beginning of the diffuse double layer. Solving the set of Eqs. (65)–(67) together with

$$q_{\text{eq}}(a) + q_{\text{eq}}(a+d) = 0 \tag{68}$$

gives the value of surface charge density of the particle, $q_{eq}(a)$, as function of ionic strength, pH and pK. From the same equations $\Psi_{eq}(a)$ and $\Psi_{eq}(a+d)$ can be obtained. We have yet said nothing about the zeta potential in this case. In Appendix A it was assumed that in the case of no Stern layer,

$$\Psi_{\text{eq}}(a) = \zeta \tag{69}$$

In the presence of a Stern layer it is usually assumed that

$$\Psi_{\text{eq}}(a+d) = \zeta \tag{70}$$

As d and C_{Stern} remain unknown, changing the position of the shear plane will only affect these parameters, so there is no benefit is discussing its exact position. The following example gives the surface charge of silica as function of ionic strength assuming that the Stern layer is a dielectric medium, using the following parameters, taken from [50]:

pK	$C_{Stern}(F/m^2)$	$\Gamma^0\ (nm^{-2})$
7.5	2.9	8

The traditional description of the Stern layer discussed above is to be adapted when an electric field is applied to the system. It is then usually assumed that (part of) ions are mobile within the Stern layer in reaction to the applied electric field. This implies that the Stern layer is not a pure dielectric medium, and that a Stern layer conductance should be accounted for.

A Stern layer conductivity can easily be added to the dipolar coefficient Eq. (3), following the procedure given in the Shell model subsection. This leads to the new dipolar coefficient [48]:

$$\tilde{\beta}(\omega) = \frac{\tilde{\sigma}_g - \tilde{\sigma}_e + \sigma_{//}(1 - J_1/J_2) + \tilde{\sigma}_{//}^{\text{St}} + \tilde{\sigma}_{\perp}^{\text{St}}/2}{\tilde{\sigma}_g + 2\tilde{\sigma}_e + \sigma_{//}(1 + 2J_1/J_2) + \tilde{\sigma}_{//}^{\text{St}} - \tilde{\sigma}_{\perp}^{\text{St}}} \tag{71}$$

where $\tilde{\sigma}_{//}^{\text{St}}$ and $\tilde{\sigma}_{\perp}^{\text{St}}$ are the (complex) conductivities for the Stern layer parallel and perpendicular to the particle's surface. By fitting data on suspensions, it was found that

$$\tilde{\sigma}_{//}^{\text{St}} = \tilde{\sigma}_{\perp}^{\text{St}} = \text{St} \times \sigma_e \tag{72}$$

where St is a real coefficient, which make both $\tilde{\sigma}_{//}^{\text{St}}$ and $\tilde{\sigma}_{\perp}^{\text{St}}$ real variables. This choice gives the same local field as when no Stern layer is introduced and corresponds to what many authors do: St is similar to the Θ_2 introduced in [31] and similar coefficients have been used by [52,53].

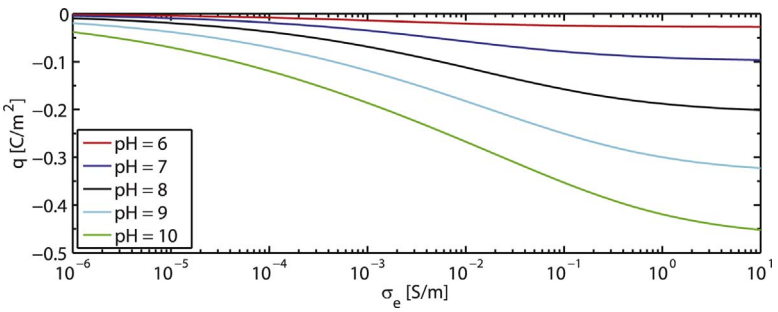

Fig. 10. Surface charge densities of silica for different pH as a function of the conductivity of the electrolyte.

Appendix D. The Schwartz model

Schwartz [12] was one of the first with O'Konski [14] to develop models for the polarization of colloids. Schwartz's model is still widely used in the current models of the conductivity of granular material (e.g. [2]). However the model of Schwartz, when applied to the polarization of a double layer, is by construction limited to frequencies such that $f \gg f_a$ where f_a is defined in the introduction. As discussed by Lyklema et al. [54], Schwartz attributed the double-layer polarization entirely to counterions bound to the spherical particle in a thin layer. Exchange between the bulk and the layer of surface conductivity was assumed to be absent. This explains why the contribution $\widetilde{\sigma}_\perp$ which appears in Eq. (3) is not apparent in the derivation of Schwartz. Without re-deriving the model found by Schwartz, we will here only show where the differences between the full model (as found by numerical integration, and correctly reproduced by Eq. (3)) and the model of Schwartz arise. For derivation details, we refer to [12,21].

An alternating electric field $\mathbf{E}_{ext}$ of frequency ω is applied along the z-axis. Because of symmetry, spherical coordinates are chosen. The ionic density $\widetilde{n}_k$ (number /m^3) of ion k and the electric potential $\widetilde{\Psi}$ (V) can expressed as perturbation around their equilibrium values $n_{k,eq}$ and Ψ_{eq} (the equilibrium is defined as the situation when no electric field is applied):

$$\begin{aligned}\widetilde{n}_k &= n_{k,\mathrm{eq}} + \delta\widetilde{n}_k \exp(i\omega t)\cos(\theta)\\ \widetilde{\Psi} &= \Psi_{\mathrm{eq}} + \delta\widetilde{\Psi}\exp(i\omega t)\cos(\theta)\end{aligned} \tag{73}$$

To first order in the perturbation (neglecting the small products like $\delta\widetilde{n}_k\delta\widetilde{\Psi}$ terms) the ionic fluxes are given by

$$\widetilde{\mathbf{J}}_k = -\frac{D_k n_{k,\mathrm{eq}}}{\mathrm{kT}}\nabla\left(\mathrm{kT}\frac{\delta\widetilde{n}_k\cos(\theta)}{n_{k,\mathrm{eq}}} + z_k e\delta\widetilde{\Psi}\cos(\theta)\right) \tag{74}$$

where D_k is the ionic diffusion of ion k and z_k its valence, e is the absolute value of the electron charge. The conservation equation yields:

$$\frac{\partial\widetilde{n}_k}{\partial t} + \nabla\cdot\widetilde{\mathbf{J}}_k = 0 \tag{75}$$

From Eqs. (74) and (75), we obtain:

$$i\omega\delta\widetilde{n}_k\cos(\theta) = D_k\nabla\cdot\left[n_{k,\mathrm{eq}}\nabla\left(\frac{\delta\widetilde{n}_k\cos(\theta)}{n_{k,\mathrm{eq}}} + \frac{z_k e}{\mathrm{kT}}\delta\widetilde{\Psi}\cos(\theta)\right)\right] \tag{76}$$

Each of the last two equations ($k = +$, $k = -$) depends on the parallel (along r) and perpendicular (along θ) to the electric field direction:

$$\nabla = \nabla_r + \nabla_\theta \tag{77}$$

In Schwartz' model there is no dependence of the variables on r implying that the term in ∇_r is zero. For distances close to $r = a$ one finds, for the ion k which represents the counterion:

$$\begin{aligned}i\omega\delta\widetilde{n}_k\cos(\theta) &= D_k n_{k,\mathrm{eq}}\nabla_\theta\cdot\left[\nabla_\theta\left(\frac{\delta\widetilde{n}_k}{n_{k,\mathrm{eq}}}\cos(\theta) + \frac{z_k e}{\mathrm{kT}}\delta\widetilde{\Psi}\cos(\theta)\right)\right]\\ &= \frac{D_k}{a^2}\frac{n_{k,\mathrm{eq}}}{\sin(\theta)}\frac{\partial}{\partial\theta}\left[\sin(\theta)\frac{\partial}{\partial\theta}\left(\frac{\delta\widetilde{n}_k}{n_{k,\mathrm{eq}}}\cos(\theta) + \frac{z_k e}{\mathrm{kT}}\delta\widetilde{\Psi}\cos(\theta)\right)\right]\end{aligned} \tag{78}$$

This last equation is Eq. (15) in the paper of Schwartz [12]. Re-arranging this equation leads to:

$$\left[\frac{i\omega a^2}{2D_k} + 1\right]\frac{\delta\widetilde{n}_k}{n_{k,\mathrm{eq}}} = -\frac{z_k e}{\mathrm{kT}}\delta\widetilde{\Psi} \tag{79}$$

One can then define a characteristic time τ_k and frequency ω_k (similar to the frequency $\omega_a = 2\pi f_a$ defined in the introduction)

$$\omega_k = \frac{2D_k}{a^2} = \frac{1}{\tau_k} \tag{80}$$

This is the time τ_k defined by Eq. (50) in [28] and by Eq. (21) in [54]. Note, however, that Lyklema et al. [54] (as we do) use the bulk diffusion coefficient D_k whereas Leroy et al. [28] introduce a "known Stern layer diffusion coefficient" (text under their Eq. (50)) as Leroy et al. [28] that consider a particle with a polarizable Stern layer and no diffuse layer. In a later article by the same research group, see [2], the authors state that "Surface conductivity corresponds to the electrical conduction in the electrical double layer coating the surface of the grains. Apparently, two contributions can therefore coexist. The first is the electrical conduction in the diffuse layer and the second is the electrical contribution of the Stern layer as described for instance in the dynamic Stern layer model of [3]." In fact the standard models for the polarization of a charged colloidal particle in an electrolyte usually only consider the polarization of the double layer, which leads to the surface conductivities $\widetilde{\sigma}_\perp$ and $\widetilde{\sigma}_\perp$ in Eq. (3). The inclusion of a Stern layer conductivity can be done by adapting the boundary at the particle's surface [55,3], or by the analytical methods detailed in Appendix C. In the present subsection, we apply Schwartz model to the polarization of the double layer only, and we do not consider a Stern layer.

Eq. (74) yields for the case considered by Schwartz:

$$\widetilde{J}_k = -\frac{D_k}{a}\left(\frac{\partial}{\partial\theta}[\delta\widetilde{n}_k\cos(\theta)] + \frac{z_k e}{\mathrm{kT}}n_{k,\mathrm{eq}}\frac{\partial}{\partial\theta}[\delta\widetilde{\Psi}\cos(\theta)]\right) \tag{81}$$

From Eq. (79) one gets

$$\delta\widetilde{n}_k\cos(\theta) = \frac{-n_{k,\mathrm{eq}}}{i\omega\tau_k + 1}\frac{z_k e}{\mathrm{kT}}\delta\widetilde{\Psi}\cos(\theta) \tag{82}$$

This equation is similar to Eq. (49) in [28]. Combining Eqs. (81) and (82) we obtain:

$$e\widetilde{J}_k = -\frac{z_k e^2 D_k}{\mathrm{kT}} n_{k,\mathrm{eq}} \left(\frac{i\omega\tau_k}{i\omega\tau_k + 1}\right) \frac{1}{a}\frac{\partial}{\partial\theta}[\delta\widetilde{\Psi}\cos(\theta)]$$
$$= \frac{z_k e^2 D_k}{\mathrm{kT}} n_{k,\mathrm{eq}} \left(\frac{i\omega\tau_k}{i\omega\tau_k + 1}\right) \widetilde{E}_\theta \tag{83}$$

The electric field $\widetilde{E}_\theta$ is the local electric field in the vicinity of the particle due to the application of the electric field. It is from this last equation that most authors define their surface conductivity, see for example Eqs. (55) and (56) in Leroy et al. [28]. Following these authors we define a complex surface conductivity Σ_S^*:

$$e\widetilde{J}_k = \Sigma_S^* \widetilde{E}_\theta$$
$$\Sigma_S^* = \frac{z_k e^2 D_k}{\mathrm{kT}} n_{k,\mathrm{eq}}(a) \left(\frac{i\omega\tau_k}{i\omega\tau_k + 1}\right) \tag{84}$$

Contrary to the expression for the surface conductivity $\sigma_{//}$ we gave in Eq. (4), Σ_S^* is a complex number and frequency-dependent. The reason is that Σ_S^* contains terms proportional to both $\sigma_{//}$ and $\widetilde{\sigma}_\perp$. By accounting for both the parallel (along r) and perpendicular (along θ) component in Eq. (76), it possible to evaluate completely the ionic fluxes. For the full analytical derivation, we refer to [21]. The equivalence between Σ_S^* and $\sigma_{//}$ can however be made in the special case of frequencies such that $\omega \gg 1/\tau_k$. In that case the polarization of the double layer is mainly due to the movement of ions in the θ direction (parallel to the particle's surface) and there is nearly no influx of ions from the r direction perpendicular to the surface ($\widetilde{\sigma}_\perp \simeq 0$) that would lead to an additional contribution in the parallel direction. Eq. (84) gives for $\omega \gg 1/\tau_k$, assuming as in the previous section that $|z_k| = 1$ and $D_k = D$

$$\Sigma_S^* \to \frac{e^2 D}{\mathrm{kT}} n_{k,\mathrm{eq}}(a) \tag{85}$$

A relation between surface charge $q_{eq}(a)$ and zeta potential is given in Eq. (55) of Appendix B. Using the fact that for an infinitely thin double layer, one has in good approximation $q_{eq}(a) \simeq e a n_{k,eq}(a)$ (where ion k represents the counterion) and we obtain:

$$n_{k,\mathrm{eq}}(a) \simeq n_\infty \frac{2}{\kappa a} \exp\left(\frac{e\Psi_{\mathrm{eq}}(a)}{2\mathrm{kT}}\right) \tag{86}$$

As, by definition,

$$\sigma_e = \frac{2e^2 n_\infty D}{\mathrm{kT}} \tag{87}$$

we deduce that

$$\Sigma_S^* = \sigma_{//}/2 \ (\text{for } \omega \gg 1/\tau_k) \tag{88}$$

The factor 2 appears because in Eq. (84) only counterions were considered, and that by definition the ionic conductivity σ_e depends on both co- and counterions (hence the 2 in Eq. (87)). In the present article, we have adopted the definition of $\sigma_{//}$ used by a large community of colloid scientists, however, in [21] a different definition was used, in which case Eq. (88) would reduce to $\Sigma_S^* = \sigma_{//}$ (for $\omega \gg 1/\tau_k$).

References

[1] K. Koch, A. Revil, K. Holliger, Relating the permeability of quartz sands to their grain size and spectral induced polarization characteristics, Geophys. J. Int. 190 (2012) 230–242.
[2] A. Revil, N. Florsch, Determination of permeability from spectral induced polarization in granular media, Geophys. J. Int. 181 (3) (2010) 1480–1498.
[3] C.F. Zukoski, D.A. Saville, The interpretation of electrokinetic measurements using a dynamic model of the stern layer: I. The dynamic model, J. Colloid Interface Sci. 114 (1) (1986) 32–44.
[4] G.E. Archie, The electrical resistivity log as an aid in determining some reservoir characteristics, Trans. AIME 146 (01) (1942) 54–62.
[5] D.P. Lesmes, F.D. Morgan, Dielectric spectroscopy of sedimentary rocks, J. Geophys. Res. 06 (B7) (2001) 13329–13346.
[6] P.W.J. Glover, P.G. Meredith, P.R. Sammonds, S.A.F. Murrell, Ionic surface electrical conductivity in sandstone, J. Geophys. Res. 99 (B11) (1994) 21635–21650.
[7] A. Binley, L. Slater, M. Fukes, G. Cassiani, The relationship between spectral induced polarization and hydraulic properties of saturated and unsaturated sandstone, Water Resour. 41 (2005) W12417.
[8] W.H. Pelton, S.H. Ward, P.G. Hallof, W.R. Sill, P.H. Nelson, Mineral discrimination and removal of inductive coupling with multifrequency IP, Geophysics 43 (3) (1978) 588–609.
[9] P.N. Sen, C. Scala, M.H. Cohen, A self-similar model for sedimentary rocks with application to the dielectric constant of fused glass beads, Geophysics 46 (5) (1981) 781.
[10] C. Grosse, A.V. Delgado, Dielectric dispersion in aqueous colloidal systems, Curr. Opin. Colloid Interface Sci. 15 (3) (2010) 145–159.
[11] A. Revil, On charge accumulation in heterogeneous porous rocks under the influence of an external electric field, Geophysics 78 (4) (2013) D271–D291.
[12] G. Schwartz, A theory of the low-frequency dielectric dispersion of colloidal particles in electrolyte solution, J. Phys. Chem. 66 (12) (1962) 2636–2642.
[13] C.T. O'Konski, Effect of interfacial conductivity on dielectric properties, J. Chem. Phys. 23 (8) (1955) 1559.
[14] C.T. O'Konski, Electric properties of macromolecules. V. Theory of ionic polarization in polyelectrolytes, J. Phys. Chem. 64 (5) (1960) 605–619.
[15] M. Fixman, Charged macromolecules in external fields. I. The sphere, J. Chem. Phys. 72 (9) (1980) 5177–5186.
[16] M. Fixman, Thin double layer approximation for electrophoresis and dielectric response, J. Chem. Phys. 78 (3) (1983) 1483–1491.
[17] E.J. Hinch, J.D. Sherwood, W.C. Chew, P.N. Sen, Dielectric response of a dilute suspension of spheres with thin double layers in an asymmetric electrolyte, J. Chem. Soc. Faraday Trans. 2: Mol. Chem. Phys. 80 (5) (1984) 535–551.
[18] R.W. O'Brien, The response of a colloidal suspension to an alternating electric field, Adv. Colloid Interface Sci. 16 (1) (1982) 281–320.
[19] R.W. O'Brien, The high-frequency dielectric dispersion of a colloid, J. Colloid Interface Sci. 113 (1) (1986) 81–93.
[20] E.H. DeLacey, L.R. White, Dielectric response and conductivity of dilute suspensions of colloidal particles, J. Chem. Soc. Faraday Trans. 2: Mol. Chem. Phys. 77 (11) (1981) 2007–2039.
[21] C. Chassagne, D. Bedeaux, The dielectric response of a colloidal spheroid, J. Colloid Interface Sci. 326 (1) (2008) 240–253.
[22] L.A. Rosen, D.A. Saville, Dielectric spectroscopy of colloidal dispersions: comparisons between experiment and theory, Langmuir 7 (1991) 36–42.
[23] R.W. O'Brien, W.N. Rowlands, Measuring the surface conductance of kaolinite particles, J. Colloid Interface Sci. 159 (2) (1993) 471–476.
[24] W.N. Rowlands, R.W. O'Brien, The dynamic mobility and dielectric response of kaolinite particles, J. Colloid Interface Sci. 175 (1995) 190–200.
[25] M. Rasmusson, W. Rowlands, R.W. O'Brien, R.J. Hunter, The dynamic mobility and dielectric response of sodium bentonite, J. Colloid Interface Sci. 189 (1997) 92–100.
[26] M. Kosmulski, P. Dahlsten, High ionic strength electrokinetics of clay minerals, Colloids Surf. A: Physicochem. Eng. Aspects 291 (2006) 212–218.
[27] A.E. Bussian, Electrical conductance in a porous medium, Geophysics 48 (9) (1983) 1258–1268.
[28] P. Leroy, A. Revil, A. Kemna, P. Cosenza, A. Ghorbani, Complex conductivity of water-saturated packs of glass beads, J. Colloid Interface Sci. 321 (1) (2008) 103–117.

[29] J.J. Bikerman, Electrokinetic equations and surface conductance. A survey of the diffuse double layer theory of colloidal solutions, Trans. Faraday Soc. 36 (1940) 154–160.
[30] S.S. Dukhin, V.N. Shilov, Dielectric Phenomena and the Double Layer in Disperse Systems and Polyelectrolytes, Wiley, 1974.
[31] J. Lyklema, M. Minor, On surface conduction and its role in electrokinetics, Colloids Surf. A: Physicochem. Eng. Aspects 140 (1) (1998) 33–41.
[32] H.J. Vinegar, M.H. Waxman, Induced polarization of shaly sands, Geophysics 49 (8) (1984) 1267–1287.
[33] J.H. Börner, V. Herdegen, J.-U. Repke, K. Spitzer, Spectral induced polarization of the three-phase system CO_2–brine–sand under reservoir conditions, Geophys. J. Int. 208 (1) (2017) 289–305.
[34] A. Revil, L.M. Cathles, Permeability of shaly sands, Water Resour. Res. 35 (3) (1999) 651–662.
[35] A. Bolève, A. Crespy, A. Revil, F. Janod, J.L. Mattiuzzo, Streaming potentials of granular media: influence of the Dukhin and Reynolds numbers, J. Geophys. Res. 112 (1) (2007) B08204.
[36] L.D. Slater, D.R. Glaser, Controls on induced polarization in sandy unconsolidated sediments and application to aquifer characterization, Geophysics 68 (2003) 1547–1588.
[37] A. Revil, P. Kessouri, C. Torres-Verden, Electrical conductivity, induced polarization, and permeability of the Fontainebleau sandstone, Geophysics 79 (5) (2014) D301–D318.
[38] A. Weller, K. Breede, L. Slater, S. Nordsiek, Effect of changing water salinity on complex conductivity spectra of sandstones, Geophysics 76 (5) (2011) F315–F327.
[39] C. Chassagne, E. Dubois, M.L. Jiménez, J.M. Van Der Ploeg, J. Van Turnhout, Compensating for electrode polarization in dielectric spectroscopy studies of colloidal suspensions: theoretical assessment of existing methods, Front. Chem. 4 (30) (2016).
[40] E. Zimmermann, A. Kemna, J. Berwix, W. Glaas, H. Münch, J. Huisman, A high-accuracy impedance spectrometer for measuring sediments with low polarizability, Meas. Sci. Technol. 19 (2008) 105603.
[41] Q. Niu, A. Revil, M. Saidian, Salinity dependence of the complex surface conductivity of the Portland sandstone, Geophysics 81 (2) (2016) D125–D140.
[42] C.J.F. Böttcher, O.C. van Belle, P. Bordewijk, A. Rip, Theory of Electric Polarization vol. 2, Elsevier Science Ltd., 1978.
[43] H. Ohshima, The Donnan potential-surface potential relationship for a cylindrical soft particle in an electrolyte solution, J. Colloid Interface Sci. 323 (2008) 313–316.
[45] C. Chassagne, F. Mietta, J.C. Winterwerp, Electrokinetic study of kaolinite suspensions, J. Colloid Interface Sci. 336 (2009) 352–359.
[46] J.A. Reynolds, J.M. Hough, Formulae for dielectric constant of mixtures, Proc. Phys. Soc. B 70 (8) (1957) 769.
[47] C. Grosse, Relaxation mechanism of homogenous particles and cells suspended in aqueous electrolyte solutions, in: A.V. Delgado (Ed.), Interfacial Electrokinetics and Electrophoresis, Dekker, New York, NY, 2002, pp. 277–327.
[48] C. Chassagne, D. Bedeaux, G.J.M. Koper, Dielectric response of colloidal spheres in non-symmetric electrolytes, Phys. A: Stat. Mech. Appl. 317 (3) (2003) 321–344.
[49] W.B. Russel, D.A. Saville, W.R. Schowalter, Colloidal Dispersions, Cambridge University Press, Cambridge, 1989.
[50] S.H. Behrens, D.G. Grier, The charge of glass and silica surfaces, J. Chem. Phys. 115 (14) (2001) 6716–6721.
[51] H.R. Kruyt, Colloid Science, Irreversible Systems vol. I, Elsevier, 1952.
[52] J. Kijlstra, H.P. van Leeuwen, J. Lyklema, Effects of surface conduction on the electrokinetic properties of colloids, J. Chem. Soc. Faraday Trans. 88 (23) (1992) 3441–3449.
[53] L.A. Rosen, J.C. Baygents, D.A. Saville, The interpretation of dielectric response measurements on colloidal dispersions using the dynamic Stern layer model, J. Chem. Phys. 98 (5) (1993) 4183.
[54] J. Lyklema, S.S. Dukhin, V.N. Shilov, The relaxation of the double layer around colloidal particles and the low-frequency dielectric dispersion: Part I. Theoretical considerations, J. Electroanal. Chem. Interfacial Electrochem. 143 (1) (1983) 1–21.
[55] C.S. Mangelsdorf, L.R. White, The dynamic double layer – Part 1 – Theory of a mobile Stern layer, J. Chem. Soc. Faraday Trans. 94 (16) (1998) 2441–2452.